Research Square

Preprints are preliminary reports that have not undergone peer review.
They should not be considered conclusive, used to inform clinical practice,
or referenced by the media as validated information.

Hydrastinine and β-sitosterol Synergistically Target Acute Myelocytic Leukemia in a Ferroptosis-Related Prognostic Model

Shuyao Yang
Dalian Medical University
Xiangbo Lin
Dalian Medical University
Bo Shi
Dalian Medical University
Jiaqi Meng
Dalian Medical University
Liang Liu
The Second Affiliated Hospital of Dalian Medical University
Lina Yan
The Second Affiliated Hospital of Dalian Medical University
Fang Xie (xfang1101@dmu.edu.cn)
Dalian Medical University

Research Article

Keywords: AML, ferroptosis, prognosis, immune infiltration, integrated traditional and western medicine, synergy effect

Posted Date: December 20th, 2023

DOI: https://doi.org/10.21203/rs.3.rs-3770830/v1

License: This work is licensed under a Creative Commons Attribution 4.0 International License.
Read Full License

Additional Declarations: No competing interests reported.

Abstract

Acute myeloid leukemia (AML) is a malignant tumor with a high incidence and poor prognosis. Ferroptosis plays a crucial role in regulating carcinogenesis and tumor progression. However, a combination therapy of traditional Chinese medicine and western medicine targeting AML using a ferroptosis-related prognostic model is lacking. Herein, β-sitosterol and hydrastinine were shown to exert a significant synergistic effect on AML. First, prognostic genes associated with ferroptosis were evaluated and the prognosis model was obtained by bioinformatics. Second, the results of immune infiltration analysis showed that the abundances of B cells, macrophages, T cells and monocytes were significantly different between the high- and low-risk groups. Notably, these genes were associated with 296 drugs in the CellMiner database. Network pharmacology and molecular docking analyses showed that β-sitosterol, the active ingredient in Tripterygium wilfordii, targeted oncogenes, CAS9 and PON1. Combinatorial experiments further supported that hydrastinine and β-sitosterol significantly inhibited the growth of AML cells and improved the drug sensitivity of AML cells to ferroptosis inducers. In conclusion, our findings provide a potential strategy for the combined treatment of AML for integrative medicine.

1. Introduction

Acute myeloid leukemia (AML) is an extremely dangerous blood disorder, which occurs due to the malignant proliferation of myeloid stem cells in the hematopoietic system [1]. In 2016, the World Health Organization classified AML into the four following types: AML with myelodysplasia-related changes, AML with reproducible genetic abnormalities, treatment-related myeloid neoplasms, and non-specific AML [2]. AML is significantly heterogeneous, and the median survival of these patients is only four months [3]. According to statistics in the US, more than 20,000 new AML cases were reported in 2019, half of whom died and the five-year survival rate was only 28.3% [1]. The currently available treatment options for AML include chemoradiation, radiotherapy, targeted therapy, immune therapy, and stem cell therapy [4]. Among these, induction chemotherapy and hematopoietic stem-cell transplant are the most commonly used strategies in clinical practice. The long-term prognosis of patients with AML remains a cause of concern, despite the continuous improvement in treatment options [5]. In the last few years, research into the molecular heterogeneity and nosogenesis of AML has progressed, along with the improvement in the development of new drugs. However, the majority of AML patients are not cured, and treatment resistance and high relapse rates remain significant problems. Consequently, it is urgent to find new molecular mechanisms for providing more effective options for the precision treatment of AML patients and improving their survival and quality of life [6, 7].

Ferroptosis was first reported by Stockwell in 2012 [8]. It is a novel iron-dependent form of regulated cell death. It is distinct from apoptosis, cellular necrosis, and autophagy, owing to the oxidation of the accumulated oxidized lipid oxides by ferrous ions to produce reactive oxygen species, which damage the plasma membrane, eventually leading to cell death [9]. Ferroptosis occurs in the two following ways: inhibition of the system xc − and glutathione peroxidase 4 (GPX4) and induction of lipid peroxidation or mitochondrial dysfunction [10]. Ferroptosis is associated with various tumor types and treatment

responses. Cancer cells contain higher levels of iron compared to normal cells [11]. Iron homeostasis occurs abnormally in breast, ovarian, kidney, and lung cancers [12]. Inhibition of [Fe-S] cluster biosynthetase (NFS1) stimulates the expression of transferrin receptor and downregulates intracellular ferritin, causing an iron deficient response and leading to lung cancer cell death [8]. During tumorigenesis, an essential correlation between mutations in cancer-related genes and activation of ferroptosis has been reported, which can affect the efficacy of chemotherapy, radiotherapy, and immunotherapy [13], and thus, the use of drugs that target ferroptosis signaling pathways can improve the effectiveness of disease treatment. Ferroptosis plays a significant role in the progression of AML and resistance to treatment [14, 15]. Patients with leukemia have higher than normal total iron levels due to multiple blood transfusions and are more prone to ferroptosis [16, 17]. AML patients exhibit iron accumulation and dependence like solid tumors [18–20], and serum ferritin levels in these patients are inversely correlated to their prognoses [21]. Growing evidence suggests that many inducers of ferroptosis have immense potential in tumor therapy [22, 23]. Methods of ferroptosis or ferroptosis combined with chemotherapy for AML have increasingly gained research attention. Erastin, an inducer of ferroptosis, can enhance the anti-cancer activity of cytarabine and doxorubicin [14]. Garciaz found that ionomycin, a ferroptosis inducer, disrupted mitochondrial metabolism in AML cells and reduced resistance to venetoclax in these patients [24]. Currently, cytogenetics and molecular risk levels serve as important references for the clinical diagnosis of AML [25]. Some genes associated with iron deficiency have been documented and differences in AML have been noted [26]. However, their molecular mechanisms have not been elucidated. Therefore, the development of new diagnostic and therapeutic targets for AML aimed at improving the poor long-term prognoses of these patients is necessitated.

In recent years, some traditional Chinese medicines and their active ingredients have attracted attention because of their role in inducing the apoptosis of tumor cells. Radix Tripterygium wilfordii Hook.f. (LGT), a traditional Chinese medicinal herb belonging to the genus Leigong vine and the family, Venomidae, was first recorded in the Chinese Han Dynasty, "Shennong Materia Medica", and has a medicinal history of more than 2,000 years [27]. It has a wide range of anti-inflammatory, immunosuppressive, bacteriostatic, and anti-tumor effects and shows remarkable efficacy against many diseases, including various types of cancers [28, 29]. LGT extract exerts an antitumor effect in various hematologic malignancies. Many studies have elucidated the molecular mechanism of triptolide in inducing antitumor activity [30, 31]. Triptolide induces apoptosis in leukemic mice WEHI-3 cells by blocking the G0/G1 phase [28]. Triptolide causes AML cell death by downregulating XIAP and Mcl-1[32].β-sitosterol is a valuable phytosterol derived widely from various seeds in nature but is also found in certain botanicals and shows antiproliferative effects on multiple cancers [33]. Low concentrations of β-sitosterol suppress proliferation and induce apoptosis in colon, breast, prostate, liver, and mouse fibrosarcoma cancer cells [33]. β-sitosterol is instrumental in cancer as its affects ceramide metabolism [34]. β-sitosterol extracted from Ganoderma lucidum exerts its toxicity on liver cancer cells and induces apoptosis [35]. However, its mechanism in AML has not been elucidated. Hydrastinine, the main alkaloid component in Hydrastis canadensis, can be used as a hemostatic agent. Research on its role in blood diseases is little, and it is worth exploring its function for providing new ideas for clinical treatment.

In the present study, we performed LASSO analysis to develop a predictive model using ferroptosis-associated genes in AML following the identification of differentially expressed genes (DEGs). The prognostic model could predict changes in the immune microenvironment to a certain extent, as evidenced by immune-infiltration analysis. Furthermore, β-sitosterol and hydrastinine, two natural active substances, exerted a synergistic inhibitory effect on the development of AML and enhanced the drug sensitivity of AML cells to ferroptosis inducers, thus providing new ideas for targeted therapy of AML.

2. Materials and Methods

2.1. Data Collection

TCGA-LAML dataset was used as the training set and included the mRNA sequencing data of 150 patients along with their corresponding clinical information. The GSE37642 dataset from the GPL570 platform was used as the test set and comprised 140 tumor samples.

2.2. Identification of DEGs

Rank sum tests were performed on the training dataset using R v3.6.0, and ferroptosis-related genes were screened from the literature. The data type used for DEG identification was the new TPM value–log2(TPM + 1). The data were normalized using the limma package before DEG identification. The screening criteria were as follows: log fold change ≥ 1 and adjusted P-value < 0.05. The intersection of the screened DEGs and ferroptosis-related genes was taken, and subsequently, UniCox analysis and LASSO screening were performed.

2.3. Gene Set Enrichment Analysis (GSEA)

GSEA, a method of analyzing biological processes using the theories of computer science, has been used for calculating and comparing consistent differences between two biological states. The differential enrichment analysis for intersecting genes was performed based on different signaling pathways obtained from differential analysis using the R package, clusterProfiler (v4.2.2). The gene enrichment in the corresponding pathway was considered significant at $P < 0.05$.

2.4. Development and Validation of the Prognostic Risk Model

The relationship between genes and overall survival (OS) was analyzed by LASSO-COX regression analysis. The software package, glmnet, was employed to perform LASSO analysis. The prognostic risk model for AML was established based on the LASSO risk score calculation formula. Subsequently, AML patients were divided into high- and low-risk groups according to the median risk score. The plotted KM curves were used for comparing OS between the two risk groups. For survival analysis, the SURVIVAL package in R was utilized. The reliability of the prognostic model can be accessed by the ROC curve analysis.

2.5. Estimation of Tumor-Infiltrating Immune Cells

CIBERSORT, a machine learning method for support vector regression analysis, is the most frequently used tool for assessing and analyzing immune cell infiltration. CIBERSORT was applied to assess the proportion of immune cell types between high- and low-risk groups by the Wilcoxon rank-sum test. The sum of all estimated immune cell type fractions in each sample was equal to 1.

2.6. Drug Sensitivity Screen for Therapeutic Targets

CellMiner (https://discover.nci.nih.gov/cellminer/home.do) is a database for drug susceptibility in the NCI-60 cell line. RNA-seq data and NIC-60drug z-score values were downloaded from the CellMiner database. z-score values correlate positively with drug sensitivity. FDA-approved was set as a screening condition, and Pearson correlation analysis was performed for the drug z-score value and characteristic gene expression. Pearson's correlation coefficient $|(PCC)| > 0.3$ and $P < 0.05$ were considered threshold values.

2.7. Collection of TGV Active Ingredients

Traditional Chinese Medicine Systems Pharmacology Database and Analysis Platform (TCMSP), a systemic pharmacology platform for Chinese herbal medicine, can be used to study the relationship between drugs, targets, and diseases. To obtain the active ingredients of TGV in this database, the screening criteria were set as oral bioavailability (OB) $\geq 30\%$ and drug similarity (DL) ≥ 0.18. A total of 28 active components and 496 target genes of TGV were collected.

2.8. Molecular Docking Analysis

PDB files of the proteins were downloaded from RSCB-PDB (https://www.rcsb.org/). The mol2 files of small molecules downloaded from TCMSP were converted into PDB files using Open Babel (v3.1.1). Autodock vina (v1.2.0) was used to assess molecular docking. The software was used to remove water molecules, separate proteins, add non-polar hydrogens, calculate the Gasteiger charge for the structure, and save the PDB file in the PDBQT format. Small molecules converted into the PDB format were saved as docking ligands in PDBQT format in Autodock vina (v1.2.0). The protein was used as the receptor and the active compound was the ligand for docking. For the docked results, 9 conformations each were generated. The conformation with the best affinity was chosen as the final docking and visualized in Pymol (v2.5.3).

2.9. Cell lines and Cell Culture

THP1 and Kasumi cell lines were provided by the American Type Culture Collection (ATCC). The complete medium for THP1 and Kasumi cells was RPMI-1640 medium, supplemented with 10% bovine serum albumin (FBS), 100 μg/ml penicillin, and 100 μg/ml streptomycin. The cells were grown at 37°C in a humidified atmosphere with 5% CO2.

2.10. CCK8 Assay to Detect Cell Viability

CCK8 assay was adopted for assessing cell viability. Briefly, 5x103 cells were inoculated into 96-well culture plates and allowed to adhere overnight. The cells were cultured in fresh medium containing

different concentrations of hydrastinine, CUDC-427, ASTX-660, PD183805, and β-sitosterol dissolved in DMSO (final concentration, 0.1%). After 48 h of incubation, CCK-8 was added and the absorbance at 450 nm was measured on an EnSpire® Multi-plate Reader (Perkin Elmer, USA). Each group of experiments was repeated thrice.

2.11. Iron assay

The iron assay was conducted using the iron assay kit (ab83366, Abcam, MA, USA). THP1 and Kasumi cells were cultured in a 10 cm^2 plate at a density of 5×10^6. After 24 h of incubation, the cells were treated with Hydrastinine, β-sitosterol, Erastin, RSL3, or DMSO for 12 h. The cells were then collected in 5x volumes of iron assay buffer on ice following the manufacturer's instructions. Following that, the cells were centrifuged at 13000 g for 10 min at 4℃. The supernatant was added to an iron reducer and incubated at room temperature for 30 min. Next, 100 μL of the iron probe was added and incubated at room temperature for 1 h. The absorbance at 593 nm was measured using a colorimetric microplate reader.

2.12. Statistical Analysis

Statistical analyses were performed using R v3.6.0. KM curves and log-rank tests were used to compare the OS between the two groups. Analysis of the ROC curves determined the predictive power of the model. Univariate regression analysis was used to determine independent prognostic factors. All parameters were set to default and $P < 0.05$ indicated a statistically significant difference.

3. Results

3.1. The ferroptosis-related genes in AML

Ferroptosis is crucial in AML. To investigate the ferroptosis status of AML, we performed the Cluster analysis based on the expression matrix for 259 genes related to ferroptosis in the TCGA-LAML dataset, and the patients were divided into k groups (k = 2–9) by different levels of ferroptosis. The Fig. 1 shows the flow of the whole article. According to consensus clustering, k = 2 was the most optimal (Fig. 2A, S1A, B). Differential analysis between groups 1 and 2 was performed using the limma package, and 711 up-regulated and 135 down-regulated DEGs were identified (Fig. 2B, C, S1C). Further, GSEA analysis was performed for these DEGs and found to be mainly enriched in the phagocytic vesicles and external side of the plasma membrane (Fig. 2D, S1D).

3.2. Establishment and validation of a prognostic signature based on ferroptosis-related genes

Next, 2553 AML oncogenes were obtained by univariate cox analysis (HR > 1, $p < 0.05$), and after assessing the overlapping with DEGs, 245 candidate genes were obtained (Fig. 3A). To exclude false positives, LASSO regression analysis was performed for these genes. Finally, 11 genes were identified and the risk score was calculated as follows: Risk score = 0.01628 × Expression (PPIF) + 0.16354 ×

Expression (TREML2) + 0.02348 × Expression (TCF15) + 0.00896 × Expression (IL2RA) + 0.00577 × Expression (CPEN8) + 0.28661 × Expression (CBR1) + 0.00253 × Expression (DDIT4) + 0. 10536 × Expression (UTF1) + 0. 04278 × Expression (PTP4A3) + 0. 05087 × Expression (SH3BGR) + 0. 07584 × Expression (CCDC167) (Fig. 3B-D). After setting the median risk score as the cut-off, 150 patients were divided into high- and low-risk groups (Fig. S2). In the training set, the difference in patient survival time was considered significant between the two risk groups (Fig. 3E), and the AUC value was 0.782 (Fig. 3F). These results were validated in the test set GSE37642 (Fig. 4).

3.3. The correlation between immune cell infiltration and prognostic signature in AML patients

To assess the relationship between the prognostic model and the immune microenvironment in AML, the proportion and correlation of different immune cell types in the tumor microenvironment between the high- and low-risk groups were analyzed (Fig. 5A-E). The same comparative analysis was performed between the AML and normal groups (Fig. S3). The results showed that the immune infiltration of B cells, naive cells, macrophages, M2 cells, T cells, CD4 memory resting cells, and monocytes was significantly different (Fig. 5F). The level of immune infiltration of monocytes in the high-risk group was significantly higher compared to the low-risk group (Fig. 5F and S3F). In conclusion, the changes in the immune microenvironment markedly after the development of AML, and this can be attributed to the prognostic model. In conclusion, the current results shows that the tumor immune microenvironment undergoes significant changes after the development of AML, which is significantly related to the risk model. The underlying mechanism of the results may be that characteristic genes lead to the remodeling of the immune microenvironment.

3.4. Drug sensitivity based on the prognostic signature

This prognostic model was validated in multiple datasets and had a wide range of applications. However, as a therapeutic target, its anti-tumor effects remain unclear. Therefore, it is essential to study the targeted anti-cancer drugs. Correlational analysis for the expression of the 11 genes obtained based on the GI50 data for drugs in the CellMiner database yielded 296 drugs with $p < 0.05$ and $|cor| > 0.3$. IL2RA, a type I transmembrane protein, plays an important role in AML[36]. Hydrastinine, SM-406, GDC-0152, CO-1686, CUDC-427, Sabutoclax, GSK-2194069, and ASTX-660 showed high sensitivity to IL2RA. Hydrastinine had the highest correlation coefficient with IL2RA, indicating that with the increase in IL2RA expression, the half-inhibitory concentration of the hydrastinine decreased, thus improving the therapeutic effect (Fig. 6 and S4).

3.5. Molecular docking

Traditional Chinese medicine is widely used in tumor treatment, and therefore, assessing effective and comprehensive treatment measures is necessary. The anti-AML effect of Tripterygium wilfordii has been reported. The active components of triptolide and the corresponding target genes were found using the TCMSP database (Fig. 7A), and the results showed that triptolide targeted the oncogene, TGFB1; kaempferol targeted GSTP1, and β-sitosterol targeted CASP9 and PON1 (Fig. 7B). Molecular docking can

be used for simulation of the active ingredients and assess the binding ability between the target and the effective compound. The score for triptolide and TGFB1 was − 6.2 kcal/mol, for kaempferol and GSTP1, it was − 7.3 kcal/mol, and for β-sitosterol and CASP9, it was − 7.9 kcal/mol (Fig. 7C and S5). β-sitosterol had the highest docking score with CASP9, showing the best docking performance with two targeted oncogenes. Therefore, β-sitosterol was assessed as a potential therapeutic drug.

3.6. Hydrastinine combined with β-sitosterol exerts a synergistic antitumor effect in AML

Based on the Cellminer results, the top 5 drugs with the highest cor values were selected for CCK8 experimental validation, and the results of IC50s in THP1 cells were obtained (Fig. 8A and S6). Hydrastinine had the optimal IC50 and cor values. To assess the inhibitory effect of integrative medicine on AML, the combination of hydrastinine and β-sitosterol was tested in THP1 cells. The combinatorial usage of the drugs was more effective in reducing cell viability than either alone (Fig. 8B, C). The results of the CCK8 experiments in two different cells were consistent (Fig. 8D, E).

3.7. Hydrastinine combined with β-sitosterol improves the sensitivity of ICC cells to ferroptosis inducers

Ferroptosis inducers are not effective in clinical application. However, our previous research showed that Hydrastinine and β-sitosterol could affect ferroptosis by targeting ferroptosis genes. Therefore, we further explored whether Hydrastinine and β-sitosterol can affect the ferroptosis of AML cells and the drug sensitivity of ferroptosis inducers. Erastin and RSL3 were used in the DMSO group to treat THP1 cells. Their IC50 values were 8.7 nM and 2.7 nM, respectively (Fig. 9A). However, in the combined use of Hydrastinine and β-sitosterol, the IC50 values changed to 6.8 nM and 2.1 nM, which indicated that the combined use of these two drugs increased the sensitivity of AML cells to ferroptosis inducers (Fig. 9B). Furthermore, we added ferroptosis inducers to the DMSO and combined drug group to detect the level of ions in the cells. The results showed that the combined drug group could significantly increase the level of ferroptosis in AML cells (Fig. 9C-D). The above results indicated that the combined use of Hydrastinine and β-sitosterol could enhance the sensitivity of AML cells to ferroptosis inducers.

4. Discussions

AML is the most prevalent form of leukemia in adults with extreme malignancy [37]. Current treatment for AML relies on intense chemotherapy but these patients continue to be plagued by extremely poor prognosis and high mortality rates. Treatment options for AML have changed significantly over the past decade, particularly with the advent of the concept of ferroptosis [38, 39]. Ferroptosis is a regulated form of death and its activation can be used to treat cancer, particularly malignancies resistant to conventional therapies. However, studies on ferroptosis-related genes as targets for AML diagnosis and treatment are scanty. We used LASSO analysis to establish a predictive model using ferroptosis-related genes for AML. We assessed AML typing and the level of risk factors in each type by analyzing single-cell sequencing data. Finally, we verified that β-sitosterol and hydrastinine exerted synergistic inhibition on AML cells. Our

findings offer a novel predictive model for the diagnosis of AML using ferroptosis-related genes, while also suggesting targets and potential treatment options for its treatment.

Ferroptosis is a non-apoptotic cell death form. It occurs due to the accumulation of intracellular iron leading to lipid peroxidation and increased concentration of intracellularly generated ROS at lethal levels [40, 41]. Growing evidence suggests that multiple inducers of ferroptosis have great cancer therapeutic potential [22, 42]. Daolin Tang et al. suggest that erastin, a inducer of ferroptosis, selectively enhances the sensitivity of HL-60 cells to chemotherapeutic agents in a Ras-independent manner [14]. Fei-hu Chen et al. show that ferroptosis participates in the action of ATPR-induced differentiation of AML cells [16]. We clustered the expression of 259 ferroptosis-related genes in AML, conducted differential analysis and COX univariate analysis between the two groups of patients, and trained the genes obtained by LASSO to obtain a risk score calculation formula for the model based on ferroptosis-related genes to predict the prognoses of patients. In this risk model, interestingly, 11 signature genes were associated with various cancers. For instance, PPIF, a peptidyl-prolyl cis-trans isomerase, is privy to the regulation of mPTP in mitochondria and affects cell death. It can act as a suitable therapeutic target for different diseases [43]. Trigger receptor-2 (TREM2) expressed on myeloid cells is a crucial autoimmune negative regulator. It binds to various tissue damage-related ligands and has anti-inflammatory and macrophage fusion functions. It plays an essential role in the tumor environment [44]. TCF15 is involved in early mesoderm transcriptional regulation and inhibits Id protein, rapidly downregulates Nanog, and accelerates somatic cell lineage differentiation, associated with the tumor prognosis [45]. CPNE8 belongs to the copine family and encodes a calcium-dependent protein, which is intimately linked to the occurrence of various types of tumors; it inhibits the proliferation of AML cancer cells [46]. CBR1, G protein-coupled receptor, is a subtype of the CBR family, known to exert anti-tumor effects [47]. DDIT4, a DNA damage response 1 or stress-triggered protein, can be activated under various stress conditions, and dysregulated dit4 expression has been observed in many malignancies [48]. UTF1 is expressed in early embryonic development and primordial germ cells and maintains spermatogonial stemness. It is highly expressed in cancer cells and associated with the transcriptional regulation [49]. PTP4A3, a phosphatase associated with tumor metastasis, is consistently highly expressed in tumor cells and regulates the adhesion of tumor cells to the extracellular matrix [50]. SH3BGR is localized in the matrix and participates in various life activities like protein assembly; its role in the pathogenesis of cancer, however, is unclear [51]. CCDC167 is related to cell proliferation and migration signaling and is aberrantly activated in several tumors [52]. Interestingly, interleukin-2 receptor subunit alpha (IL2RA) is a transmembrane protein, found mainly in the spleen, lymph nodes, and other tissues, Treg cells, basophils, activated T cells, and other cell surfaces [53]. IL2RA participates in the regulation of immune tolerance by affecting the activity of Treg cells. It is highly expressed in activated Treg cells, and specific antibodies kill Treg cells to relieve immunosuppression, crucial in anti-tumor therapy [54]. IL2RA promotes the proliferation of AML cells and affects chemoresistance and poor prognosis of these patients [55]. However, the clinical potential of anti-IL2RA therapy warrants further investigation. We aggregated the results from the training and test sets, performed KM survival analysis, and calculated the AUC values, which verified that the risk coefficient obtained from our prediction model was highly consistent for accurate prognoses of these patients. In

summary, we verified the utility and credibility of the model in both the training and test sets through several methods.

Infiltrating immune cells are essential in the tumor microenvironment (TME) of AML. Zhen Cai et al. found that immune-related genes in the TME were linked to AML prognosis [56]. The level of immune infiltration of naive B cells, macrophages.M2, CD4 resting memory T cells, and monocytes showed a sharp rise in the cancer group compared to the normal group. Monocytes also showed significant infiltration in the high-risk group. Naive B cells, i.e., B cells that are not stimulated by antigens, initiate the formation of adaptive immunity and are associated with an active immune tumor environment and patient prognosis [57]. Macrophage M2 is a type of macrophage which is alternatively activated. It activates immune cells to respond to pathogens. Macrophages are important in the initiation and regression phases of the inflammatory processes [58]. Resting memory T cells are a type of T cell affecting secondary immune responses. Its main surface marker is CD4, which regulates or "helps" other lymphocytes in their function [59]. Monocytes originate from hematopoietic stem cells in the bone marrow, where they develop and mature. It is an essential component of the immune system [60]. Monocytes are involved in the immune responses and induce a specific immune response of lymphocytes through antigen presentation [61]. Monocytes promote tumor cell metastasis by influencing the microenvironment [62]. Taken together, we not only could predict clinical prognosis but also reflect the immune cell infiltration status in the TME. Further investigations are warranted to assess whether the prognostic model can be used as a judgment standard for immunotherapy.

Chemotherapeutic drug sensitivity analysis showed a positive correlation between risk fraction-related genes and drug-inductive sensibility of several commonly used chemotherapeutic drugs, suggesting that our prognostic model could be used to predict chemotherapy regimens. A combination of molecular docking and network pharmacology analyses showed that β-sitosterol in triptolide targeted the AML oncogenes, CASP9 and PON1. To further expand the clinical value of our study, we selected the drugs showing the highest sensitivity, hydrastinine and β-sitosterol, for verification at the cellular level. Hydrastinine and β-sitosterol showed a synergistic effect on inhibiting AML. Since 2017, many new targeted drugs have gradually entered the clinical treatment stage for AML. The treatment plan is no longer limited to the standard "3 + 7 protocol" and allogeneic hematopoietic stem cell transplantation [63]. The novel small molecule targeted drugs, antibody drugs, immunotherapy drugs, and CAR-T immunotherapy have broad application prospects in treating AML [64]. Currently, the research and development of AML-targeted therapy mainly include three directions. The first is several small molecule targeted drugs, like IDH1/2 inhibitors, FLT3 inhibitors, BCL2 inhibitors, and XPO-1 inhibitors. The second is CAR-T therapy. The current development and application of CAR-T therapy in AML is lagging behind lymphatic and plasma cell tumors. Finally, it is the antibody drugs, including monoclonal antibodies, double antibodies, and triple antibodies [65, 66]. Notably, 30% of AML patients carry FLT3 mutations, and drugs that target FLT3 can improve the four-year survival in these patients by 16% [67]. Nevertheless, the long-term prognosis for the majority of AML patients remains poor, and the precise treatment of the disease and monitoring of immunity is incomplete. The research on analyzing the pathogenesis of AML must continue for suggesting novel treatment strategies. In recent years, the natural compounds

hydrastinine and β-sitosterol extracted from Hydrastis canadensis and LGT, respectively, have played an essential role in the treatment of diseases. Research has demonstrated that β-sitosterol inhibits the growth of cancer cells in the colon, breast, prostate, liver, and mouse fibrosarcoma but its role in AML is unclear [33]. The role of hydrastinine in tumors is largely unclear. In this study, we found that hydrastinine and β-sitosterol affected the expression of IL2RA, thereby synergistically inhibiting the occurrence and development of AML. Moreover, the combinated use of the two drugs improved the drug sensitivity of AML cells to ferroptosis inducers. Taken together, our findings provide a potent combination of TCM treatment options against AML.

5. Conclusions

In conclusion, we constructed a ferroptosis-related prognostic model in AML. Based on the prognostic model, a combination therapy of traditional Chinese medicine and western medicine was demonstrated in AML cells. Moreover, the combination of the two drugs improved the drug sensitivity of AML cells to ferroptosis inducers. Our research provides theoretical basis and potential therapeutic strategy for targeting ferroptosis in AML.

Declarations

Author contribution

S.Y.Y. was responsible for Software, Data curation and Validation. X.B.L. made the Formal analysis, Data curation and Visualization. B.S. was responsible for Formal analysis, Data curation and Validation. J.Q.M. made the Data curation. L.L. was responsible for Writing – review & editing. L.N.Y. made the Supervision. F.X. was responsible for Conceptualization, Methodology, Software, Data curation, Writing – original draft.

Data Availability

The datasets used in this study are available from the TCGA database (https://xenabrowser.net/datapages/), GEO database (https://www.ncbi.nlm.nih.gov/), the CellMiner database (https://discover.nci.nih.gov/cellminer/home.do), the TCMSP databse (https://old.tcmsp-e.com/tcmsp.php), and the RCSB PDB database (https://www.rcsb.org/).

Conflicts of Interest

The authors declare that there is no conflict of interest regarding the publication of this paper.

Funding Statement

No fundation.

Supplementary Materials

Figure S1 Ferroptosis clustering analysis of AML subgroups.

Figure S2 Construction of LASSO model

Figure S3 Differences in immune infiltration between AML and normal groups

Figure S4 CellMiner results

Figure S5 Molecular docking results

Figure S6 The CCK8 results of THP1 cells

References

1. Newell LF, Cook RJ (2021) Advances in acute myeloid leukemia, BMJ, 375 n2026
2. Arber DA, Orazi A, Hasserjian R, Thiele J, Borowitz MJ, Le Beau MM, Bloomfield CD, Cazzola M, Vardiman JW (2016) The 2016 revision to the World Health Organization classification of myeloid neoplasms and acute leukemia. Blood 127:2391–2405
3. Wu M, Li C, Zhu X (2018) FLT3 inhibitors in acute myeloid leukemia. J Hematol Oncol 11:133
4. Molica M, Breccia M, Foa R, Jabbour E, Kadia TM (2019) Maintenance therapy in AML: The past, the present and the future. Am J Hematol 94:1254–1265
5. Hu L, Liu J, Meng Y, Zheng H, Ding C, Wang H, Charwudzi A, Li M, Li J, Zhai Z, Xiong S (2021) Long non-coding RNA HOTAIR regulates myeloid differentiation through the upregulation of p21 via miR-17-5p in acute myeloid leukaemia. RNA Biol 18:1434–1444
6. Yang X, Wang J (2018) Precision therapy for acute myeloid leukemia. J Hematol Oncol 11:3
7. Liu H (2021) Emerging agents and regimens for AML. J Hematol Oncol 14:49
8. Dixon SJ, Lemberg KM, Lamprecht MR, Skouta R, Zaitsev EM, Gleason CE, Patel DN, Bauer AJ, Cantley AM, Yang WS, Morrison B, Stockwell BR (2012) Ferroptosis: an iron-dependent form of nonapoptotic cell death. Cell 149:1060–1072
9. Chen X, Yu C, Kang R, Kroemer G, Tang D (2021) Cellular degradation systems in ferroptosis. Cell Death Differ 28:1135–1148
10. Tang D, Chen X, Kang R, Kroemer G (2021) Ferroptosis: molecular mechanisms and health implications. Cell Res 31:107–125
11. Mou Y, Wang J, Wu J, He D, Zhang C, Duan C, Li B (2019) Ferroptosis, a new form of cell death: opportunities and challenges in cancer. J Hematol Oncol 12:34

12. Yoshida GJ (2017) Therapeutic strategies of drug repositioning targeting autophagy to induce cancer cell death: from pathophysiology to treatment. J Hematol Oncol 10:67
13. Chen X, Kang R, Kroemer G, Tang D (2021) Broadening horizons: the role of ferroptosis in cancer. Nat Rev Clin Oncol 18:280–296
14. Yu Y, Xie Y, Cao L, Yang L, Yang M, Lotze MT, Zeh HJ, Kang R, Tang D (2015) The ferroptosis inducer erastin enhances sensitivity of acute myeloid leukemia cells to chemotherapeutic agents. Mol Cell Oncol 2:e1054549
15. Mao C, Liu X, Zhang Y, Lei G, Yan Y, Lee H, Koppula P, Wu S, Zhuang L, Fang B, Poyurovsky MV, Olszewski K, Gan B (2021) DHODH-mediated ferroptosis defence is a targetable vulnerability in cancer. Nature 593:586–590
16. Du Y, Bao J, Zhang MJ, Li LL, Xu XL, Chen H, Feng YB, Peng XQ, Chen FH (2020) Targeting ferroptosis contributes to ATPR-induced AML differentiation via ROS-autophagy-lysosomal pathway. Gene 755:144889
17. Callens C, Coulon S, Naudin J, Radford-Weiss I, Boissel N, Raffoux E, Wang PH, Agarwal S, Tamouza H, Paubelle E, Asnafi V, Ribeil JA, Dessen P, Canioni D, Chandesris O, Rubio MT, Beaumont C, Benhamou M, Dombret H, Macintyre E, Monteiro RC, Moura IC, Hermine O (2010) Targeting iron homeostasis induces cellular differentiation and synergizes with differentiating agents in acute myeloid leukemia. J Exp Med 207:731–750
18. Cui Z, Fu Y, Yang Z, Gao Z, Feng H, Zhou M, Zhang L, Chen C (2022) Comprehensive Analysis of a Ferroptosis Pattern and Associated Prognostic Signature in Acute Myeloid Leukemia. Front Pharmacol 13:866325
19. Benadiba J, Rosilio C, Nebout M, Heimeroth V, Neffati Z, Popa A, Mary D, Griessinger E, Imbert V, Sirvent N, Peyron JF (2017) Iron chelation: an adjuvant therapy to target metabolism, growth and survival of murine PTEN-deficient T lymphoma and human T lymphoblastic leukemia/lymphoma. Leuk Lymphoma 58:1433–1445
20. Wang F, Lv H, Zhao B, Zhou L, Wang S, Luo J, Liu J, Shang P (2019) Iron and leukemia: new insights for future treatments. J Exp Clin Cancer Res 38:406
21. Lee B, Yoon K, Lee S, Kang JM, Kim J, Shim SH, Kim HM, Song S, Naka K, Kim AK, Yang HK, Kim SJ (2015) Homozygous deletions at 3p22, 5p14, 6q15, and 9p21 result in aberrant expression of tumor suppressor genes in gastric cancer. Genes Chromosomes Cancer 54:142–155
22. Cao J, Chen X, Jiang L, Lu B, Yuan M, Zhu D, Zhu H, He Q, Yang B, Ying M (2020) DJ-1 suppresses ferroptosis through preserving the activity of S-adenosyl homocysteine hydrolase. Nat Commun 11:1251
23. Ho J, Yu J, Wong SH, Zhang L, Liu X, Wong WT, Leung CC, Choi G, Wang MH, Gin T, Chan MT, Wu WK (2016) Autophagy in sepsis: Degradation into exhaustion? Autophagy, 12 1073–1082
24. Garciaz S, Guirguis AA, Muller S, Brown FC, Chan YC, Motazedian A, Rowe CL, Kuzich JA, Chan KL, Tran K, Smith L, MacPherson L, Liddicoat B, Lam EYN, Caneque T, Burr ML, Litalien V, Pomilio G, Poplineau M, Duprez E, Dawson SJ, Ramm G, Cox AG, Brown KK, Huang DCS, Wei AH, McArthur K,

Rodriguez R, Dawson MA (2022) Pharmacologic Reduction of Mitochondrial Iron Triggers a Noncanonical BAX/BAK-Dependent Cell Death. Cancer Discov 12:774–791

25. Zhou F, Chen B, Hematology (2021) 26 919–930
26. Grignano E, Birsen R, Chapuis N, Bouscary D (2020) From Iron Chelation to Overload as a Therapeutic Strategy to Induce Ferroptosis in Leukemic Cells. Front Oncol 10:586530
27. Liu Y, Zhong QX, Qiu HH, Wang G, Wang CC, Feng L, Jia XB (2017) Study on attenuating hepatotoxicity of Tripterygium wilfordii through compatibility of traditional Chinese medicine compound. Zhongguo Zhong Yao Za Zhi 42:3044–3048
28. Chan SF, Chen YY, Lin JJ, Liao CL, Ko YC, Tang NY, Kuo CL, Liu KC, Chung JG (2017) Triptolide induced cell death through apoptosis and autophagy in murine leukemia WEHI-3 cells in vitro and promoting immune responses in WEHI-3 generated leukemia mice in vivo. Environ Toxicol 32:550–568
29. Wang Z, Ravula R, Shi L, Song Y, Yeung S, Liu M et al (2016) Overcoming chemoresistance in prostate cancer with Chinese medicine Tripterygium wilfordii via multiple mechanisms. Oncotarget 7:61246–61261
30. Carter BZ, Mak DH, Schober WD, Dietrich MF, Pinilla C, Vassilev LT, Reed JC, Andreeff M (2008) Triptolide sensitizes AML cells to TRAIL-induced apoptosis via decrease of XIAP and p53-mediated increase of DR5, Blood, 111 3742–3750
31. Zhang C, Cui GH, Liu F, Wu QL, Chen Y (2006) Inhibitory effect of triptolide on lymph node metastasis in patients with non-Hodgkin lymphoma by regulating SDF-1/CXCR4 axis in vitro. Acta Pharmacol Sin 27:1438–1446
32. Kim MJ, Lee TH, Kim SH, Choi YJ, Heo J, Kim YH (2010) Triptolide inactivates Akt and induces caspase-dependent death in cervical cancer cells via the mitochondrial pathway. Int J Oncol 37:1177–1185
33. Zhao Y, Chang SK, Qu G, Li T, Cui H (2009) Beta-sitosterol inhibits cell growth and induces apoptosis in SGC-7901 human stomach cancer cells. J Agric Food Chem 57:5211–5218
34. von Holtz RL, Fink CS, Awad AB (1998) beta-Sitosterol activates the sphingomyelin cycle and induces apoptosis in LNCaP human prostate cancer cells. Nutr Cancer 32:8–12
35. Vo TK, Ta QTH, Chu QT, Nguyen TT, Vo VG (2020) Anti-Hepatocellular-Cancer Activity Exerted by beta-Sitosterol and beta-Sitosterol-Glucoside from Indigofera zollingeriana Miq. Molecules, p 25
36. Nguyen CH, Schlerka A, Grandits AM, Koller E, van der Kouwe E, Vassiliou GS, Staber PB, Heller G, Wieser R (2020) IL2RA Promotes Aggressiveness and Stem Cell-Related Properties of Acute Myeloid Leukemia. Cancer Res 80:4527–4539
37. Estey EH (2018) Acute myeloid leukemia: 2019 update on risk-stratification and management. Am J Hematol 93:1267–1291
38. Liang C, Zhang X, Yang M, Dong X (2019) Recent Progress in Ferroptosis Inducers for Cancer Therapy. Adv Mater 31:e1904197

39. Vanden Berghe T, Linkermann A, Jouan-Lanhouet S, Walczak H, Vandenabeele P (2014) Regulated necrosis: the expanding network of non-apoptotic cell death pathways. Nat Rev Mol Cell Biol 15:135–147
40. Stockwell BR, Friedmann Angeli JP, Bayir H, Bush AI, Conrad M, Dixon SJ, Fulda S, Gascon S, Hatzios SK, Kagan VE, Noel K, Jiang X, Linkermann A, Murphy ME, Overholtzer M, Oyagi A, Pagnussat GC, Park J, Ran Q, Rosenfeld CS, Salnikow K, Tang D, Torti FM, Torti SV, Toyokuni S, Woerpel KA, Zhang DD (2017) Ferroptosis: A Regulated Cell Death Nexus Linking Metabolism, Redox Biology, and Disease, Cell, 171 273–285
41. Nguyen THP, Mahalakshmi B, Velmurugan BK (2020) Functional role of ferroptosis on cancers, activation and deactivation by various therapeutic candidates-an update. Chem Biol Interact 317:108930
42. Hou W, Xie Y, Song X, Sun X, Lotze MT, Zeh HJ 3rd, Kang R, Tang D (2016) Autophagy promotes ferroptosis by degradation of ferritin. Autophagy 12:1425–1428
43. Panel M, Ruiz I, Brillet R, Lafdil F, Teixeira-Clerc F, Nguyen CT, Calderaro J, Gelin M, Allemand F, Guichou JF, Ghaleb B, Ahmed-Belkacem A, Morin D, Pawlotsky JM (2019) Small-Molecule Inhibitors of Cyclophilins Block Opening of the Mitochondrial Permeability Transition Pore and Protect Mice From Hepatic Ischemia/Reperfusion Injury, Gastroenterology, 157 1368–1382
44. Ford JW, McVicar DW (2009) TREM and TREM-like receptors in inflammation and disease. Curr Opin Immunol 21:38–46
45. Davies OR, Lin CY, Radzisheuskaya A, Zhou X, Taube J, Blin G, Waterhouse A, Smith AJ, Lowell S (2013) Tcf15 primes pluripotent cells for differentiation. Cell Rep 3:472–484
46. Zhang P, Cao X, Guan M, Li D, Xiang H, Peng Q, Zhou Y, Weng C, Fang X, Liu X, Mao H, Li Q, Liu G, Lu L (2022) CPNE8 Promotes Gastric Cancer Metastasis by Modulating Focal Adhesion Pathway and Tumor Microenvironment. Int J Biol Sci 18:4932–4949
47. Morin-Buote J, Ennour-Idrissi K, Poirier E, Lemieux J, Furrer D, Burguin A, Durocher F, Diorio C (2021) Association of Breast Tumour Expression of Cannabinoid Receptors CBR1 and CBR2 with Prognostic Factors and Survival in Breast Cancer Patients. J Pers Med, 11
48. Du F, Sun L, Chu Y, Li T, Lei C, Wang X, Jiang M, Min Y, Lu Y, Zhao X, Nie Y, Fan D (2018) DDIT4 promotes gastric cancer proliferation and tumorigenesis through the p53 and MAPK pathways. Cancer Commun (Lond) 38:45
49. Raina K, Dey C, Thool M, Sudhagar S, Thummer RP (2021) An Insight into the Role of UTF1 in Development, Stem Cells, and Cancer. Stem Cell Rev Rep 17:1280–1293
50. Lazo JS, Sharlow ER, Cornelison R, Hart DJ, Llaneza DC, Mendelson AJ, Rastelli EJ, Tasker NR, Landen CN Jr., Wipf P (2021) Credentialing and Pharmacologically Targeting PTP4A3 Phosphatase as a Molecular Target for Ovarian Cancer, Biomolecules, 11
51. Li W, Yan Q, Ding X, Shen C, Hu M, Zhu Y, Qin D, Lu H, Krueger BJ, Renne R, Gao SJ, Lu C (2016) The SH3BGR/STAT3 Pathway Regulates Cell Migration and Angiogenesis Induced by a Gammaherpesvirus MicroRNA. PLoS Pathog 12:e1005605

52. Pin-Shern H-PH, Chen NN, Yen PM-C, Chen F-W, Liu Y-W, Lin F-P, Feng S-Y, Cheng T-L, Yeh P-H, Omar HA, Jiang ZSJ-Z, Chan Y-S, Lai M-D, Wang C-Y (2021) Jui-Hsiang Hung, CCDC167 as a potential therapeutic target and regulator of cell cycle-related networks in breast cancer, Aging. 13:3
53. Durda P, Sabourin J, Lange EM, Nalls MA, Mychaleckyj JC, Jenny NS, Li J, Walston J, Harris TB, Psaty BM, Valdar W, Liu Y, Cushman M, Reiner AP, Tracy RP, Lange LA (2015) Plasma Levels of Soluble Interleukin-2 Receptor alpha: Associations With Clinical Cardiovascular Events and Genome-Wide Association Scan. Arterioscler Thromb Vasc Biol 35:2246–2253
54. Wang XX, Chen T (2018) Meta-analysis of the association of IL2RA polymorphisms rs2104286 and rs12722489 with multiple sclerosis risk. Immunol Invest 47:431–442
55. Chi Huu Nguyen AS, Grandits AM, Koller E, Emiel, van der Kouwe GS, Vassiliou PB, Staber Gerwin Heller, Rotraud Wieser, IL2RA promotes aggressiveness and stem cell-related properties of acute myeloid leukemia, cancer research, 15;80(20):4527–4539 (2020 Oct)
56. Yan H, Qu J, Cao W, Liu Y, Zheng G, Zhang E, Cai Z (2019) Identification of prognostic genes in the acute myeloid leukemia immune microenvironment based on TCGA data analysis. Cancer Immunol Immunother 68:1971–1978
57. Schaafsma E, Jiang C, Cheng C (2021) B cell infiltration is highly associated with prognosis and an immune-infiltrated tumor microenvironment in neuroblastoma. J Cancer Metastasis Treat, 7
58. Funes SC, Rios M, Escobar-Vera J, Kalergis AM (2018) Implications of macrophage polarization in autoimmunity. Immunology 154:186–195
59. Ahmadzadeh M, Hussain SF, Farber DL (2001) Heterogeneity of the memory CD4 T cell response: persisting effectors and resting memory T cells. J Immunol 166:926–935
60. Velten L, Haas SF, Raffel S, Blaszkiewicz S, Islam S, Hennig BP, Hirche C, Lutz C, Buss EC, Nowak D, Boch T, Hofmann WK, Ho AD, Huber W, Trumpp A, Essers MA, Steinmetz LM (2017) Human haematopoietic stem cell lineage commitment is a continuous process. Nat Cell Biol 19:271–281
61. Sallusto F, Lanzavecchia A (1994) Efficient presentation of soluble antigen by cultured human dendritic cells is maintained by granulocyte/macrophage colony-stimulating factor plus interleukin 4 and downregulated by tumor necrosis factor alpha. J Exp Med 179:1109–1118
62. Keirsse J, Van Damme H, Geeraerts X, Beschin A, Raes G, Van Ginderachter JA (2018) The role of hepatic macrophages in liver metastasis. Cell Immunol 330:202–215
63. Thol F, Heuser M (2021) Treatment for Relapsed/Refractory Acute Myeloid Leukemia, Hemasphere, 5 e572
64. Kayser S, Levis MJ (2018) Advances in targeted therapy for acute myeloid leukaemia. Br J Haematol 180:484–500
65. Perl AE The role of targeted therapy in the management of patients with AML. Hematol Am Soc Hematol Educ Program, 8;2017(1):54–65. (2017 Dec).
66. Fiorentini A, Capelli D, Saraceni F, Menotti D, Poloni A, Olivieri A (2020) The Time Has Come for Targeted Therapies for AML: Lights and Shadows. Oncol Ther 8:13–32

67. Leick MB, Levis MJ (2017) The Future of Targeting FLT3 Activation in AML. Curr Hematol Malig Rep 12:153–167

Figures

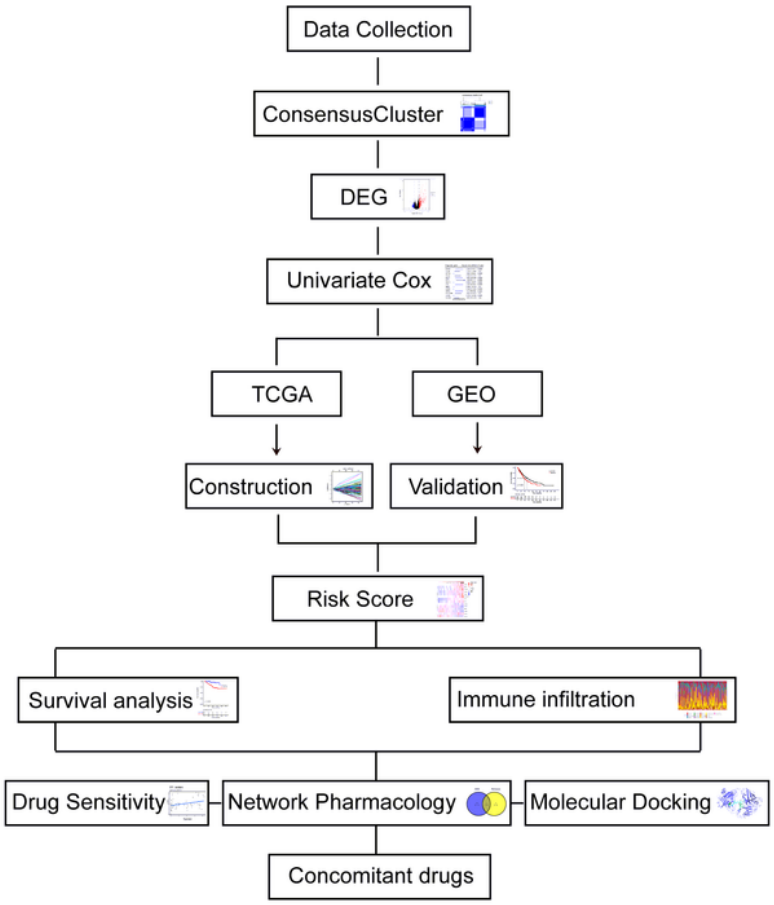


Figure 1

Flow chart of the study

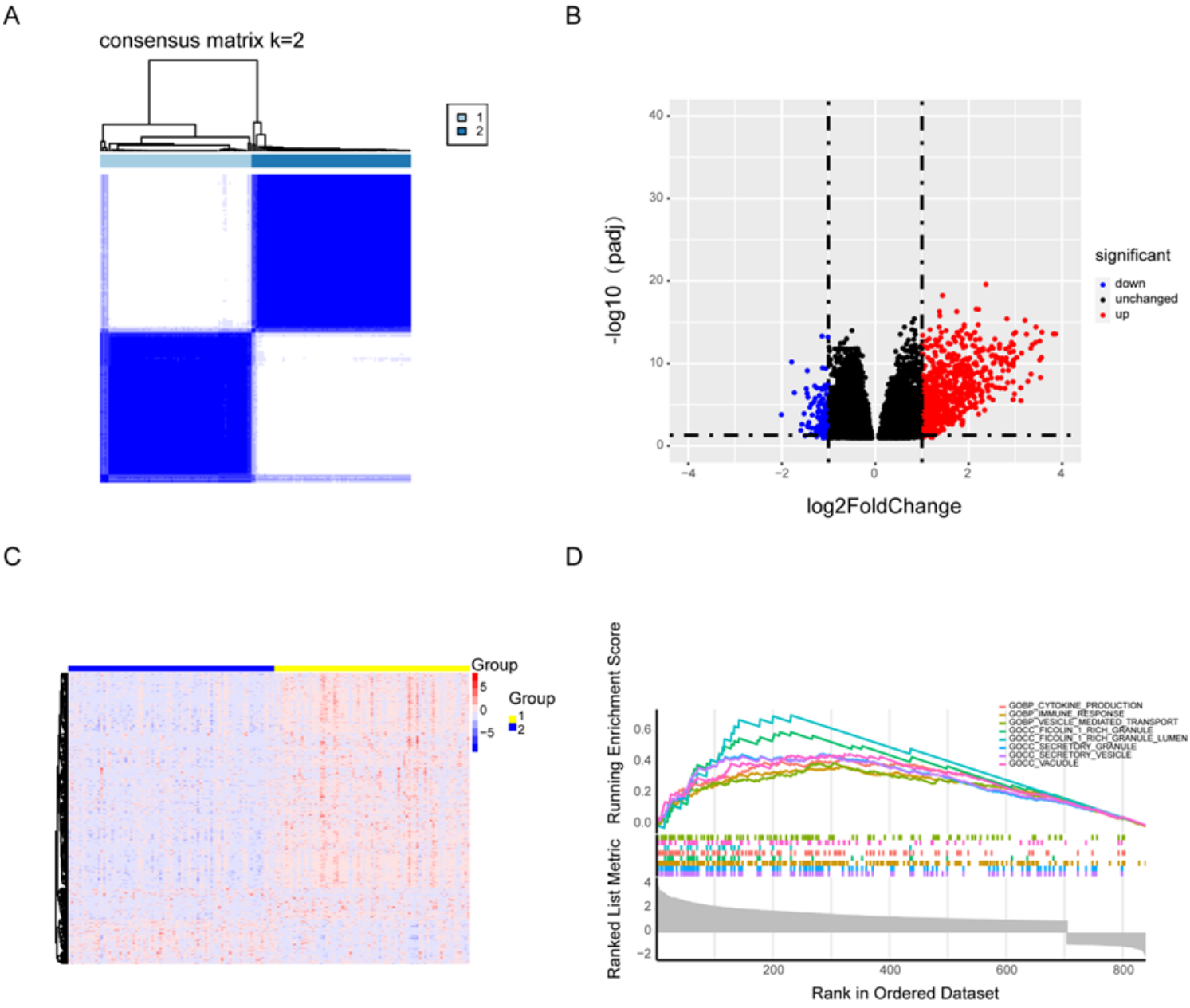


Figure 2

Cluster and differential genes analysis based on ferroptosis-related genes. (A) The consensus matrix of all samples when k = 2. (B-C) Volcano plot (B) and heatmap (C) of ferroptosis-associated DEGs between cluster 1 and cluster 2. The blue represents low-expressed DEGs and the red represents over-expressed DEGs. (D) DEGs were enriched in 8 pathways through GSEA.

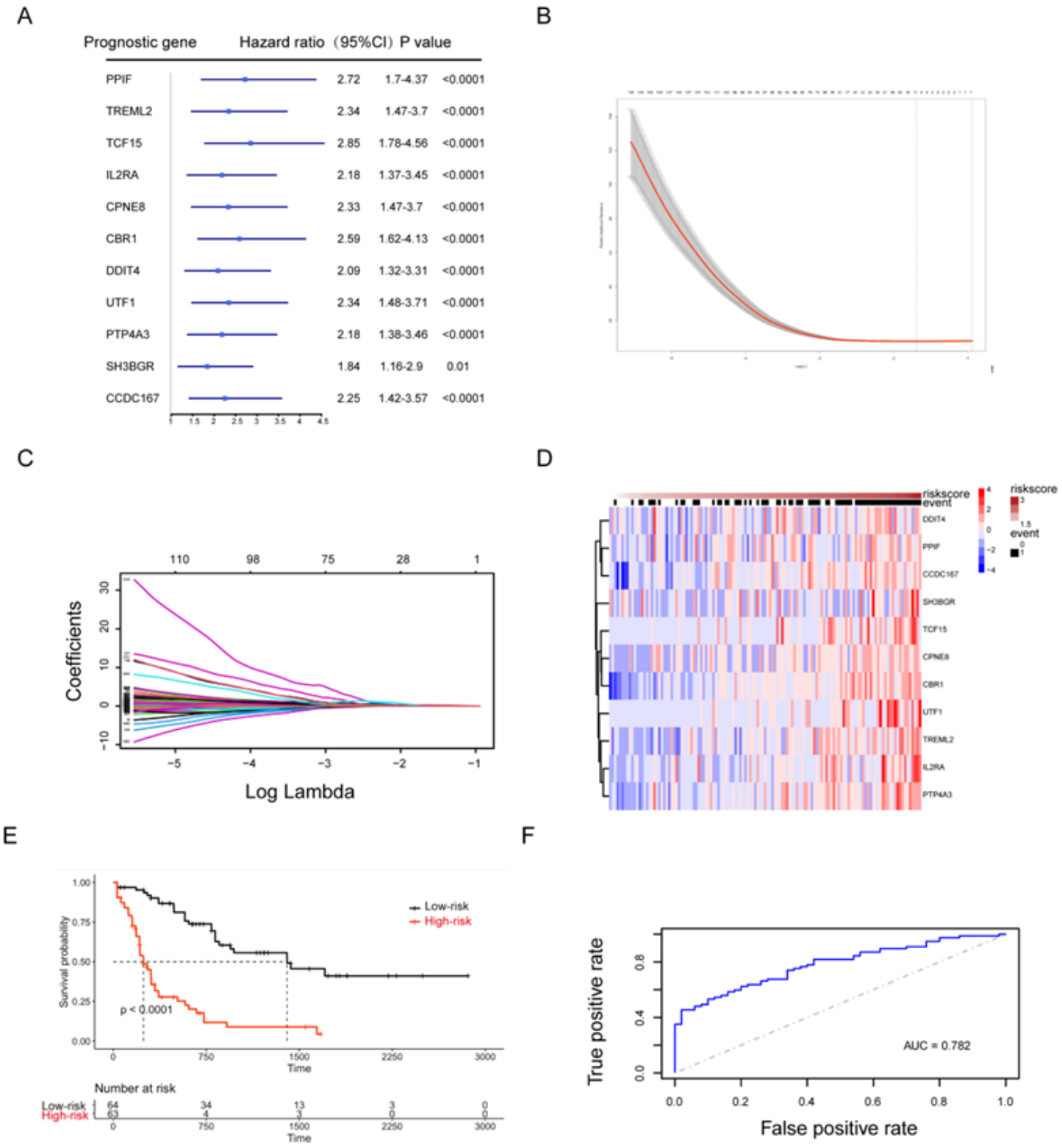


Figure 3

Construction of LASSO model. (A) The forest plot of differentially expressed mRNAs for prognosis. (B) LASSO regression coefficient profile of the 245 intersection genes. (C) LASSO deviance profile of the 245 intersection genes. (D) Heatmap of the expression values of genes with prognosis-related risk score in training set. (E) Kaplan–Meier curves of patients between high-risk score and low-risk score groups for overall survival. (F) ROC curves based on the risk score in the TCGA cohort.

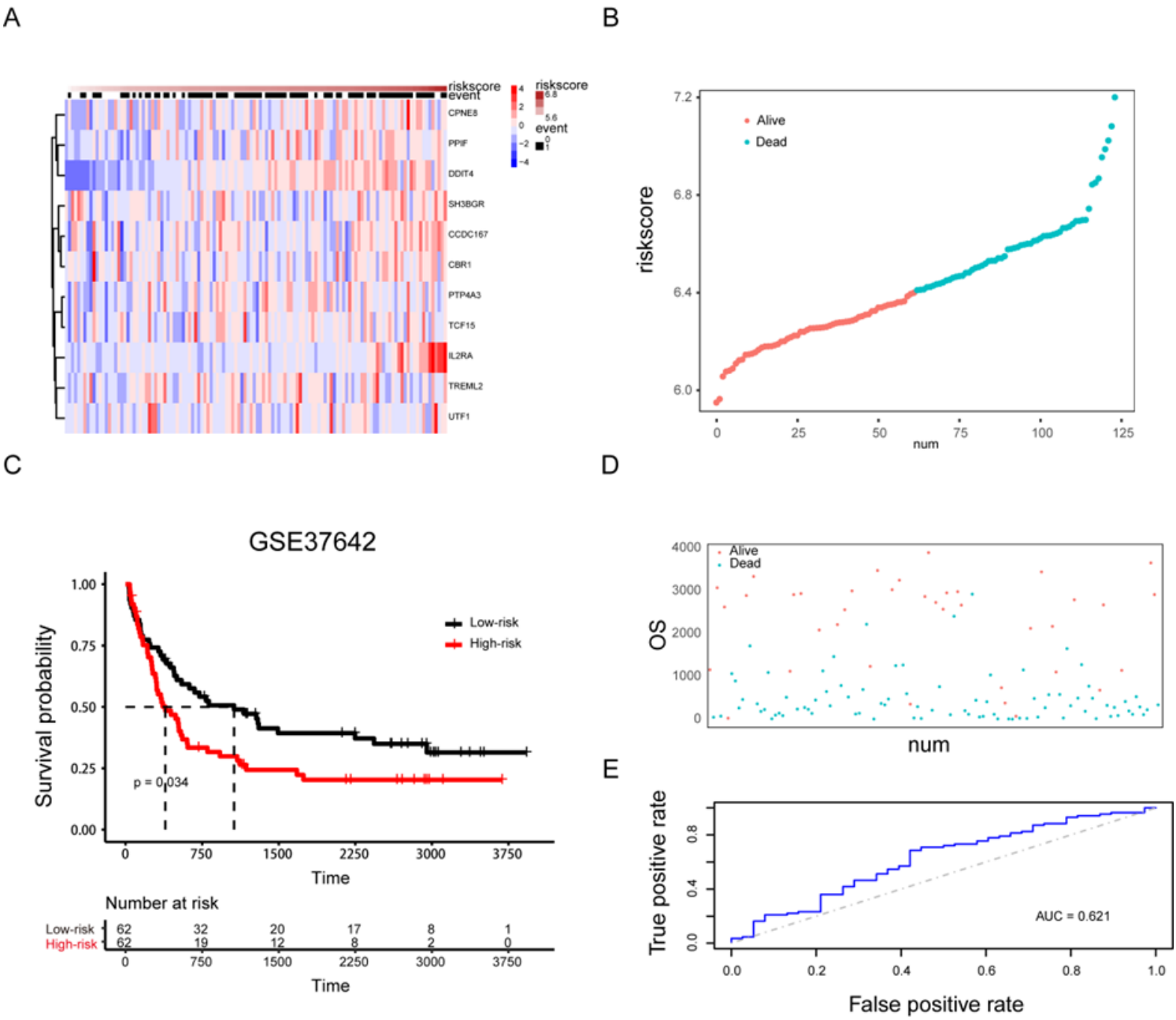


Figure 4

LASSO model validation. (A) Heatmap of the expression values of genes with prognosis-related risk score in test set. (B) The risk score distribution of patients in the test cohort. (C) Kaplan–Meier curves of patients between high-risk score and low-risk score groups for overall survival. (D) The survival status of patients in the test cohort. (E) ROC curves based on the risk score in the test cohort.

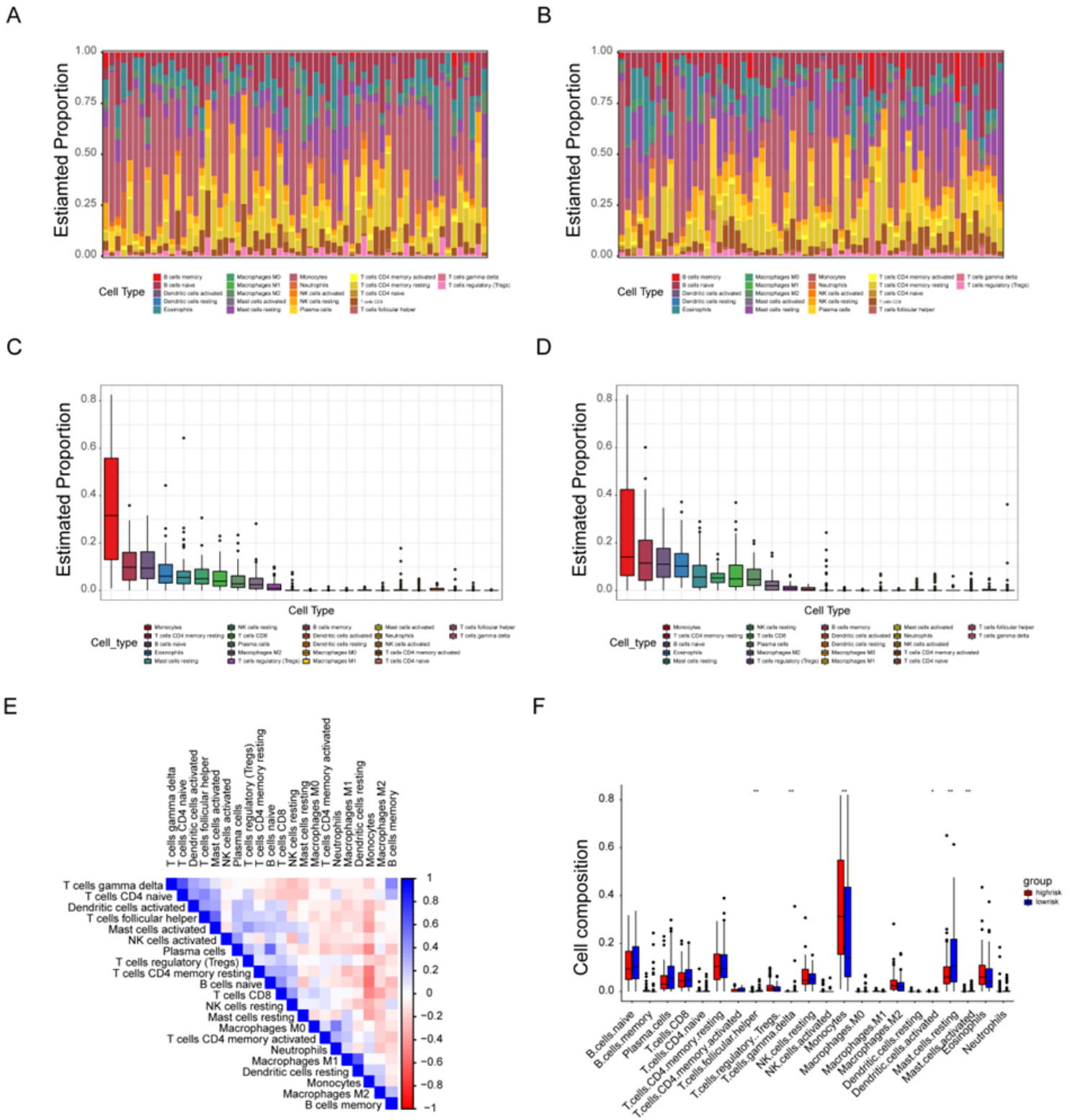


Figure 5

Differences in immune infiltration between high and low risk groups. (A-B) Distribution of various types of immune cells in high-risk group and low-risk group. (C-D) Proportion of immune cells in high-risk group and low-risk group. (E) Correlation analysis of immune cells in high-risk group and low-risk group. (F) Comparison of the proportion of immune cells in high and low risk groups.

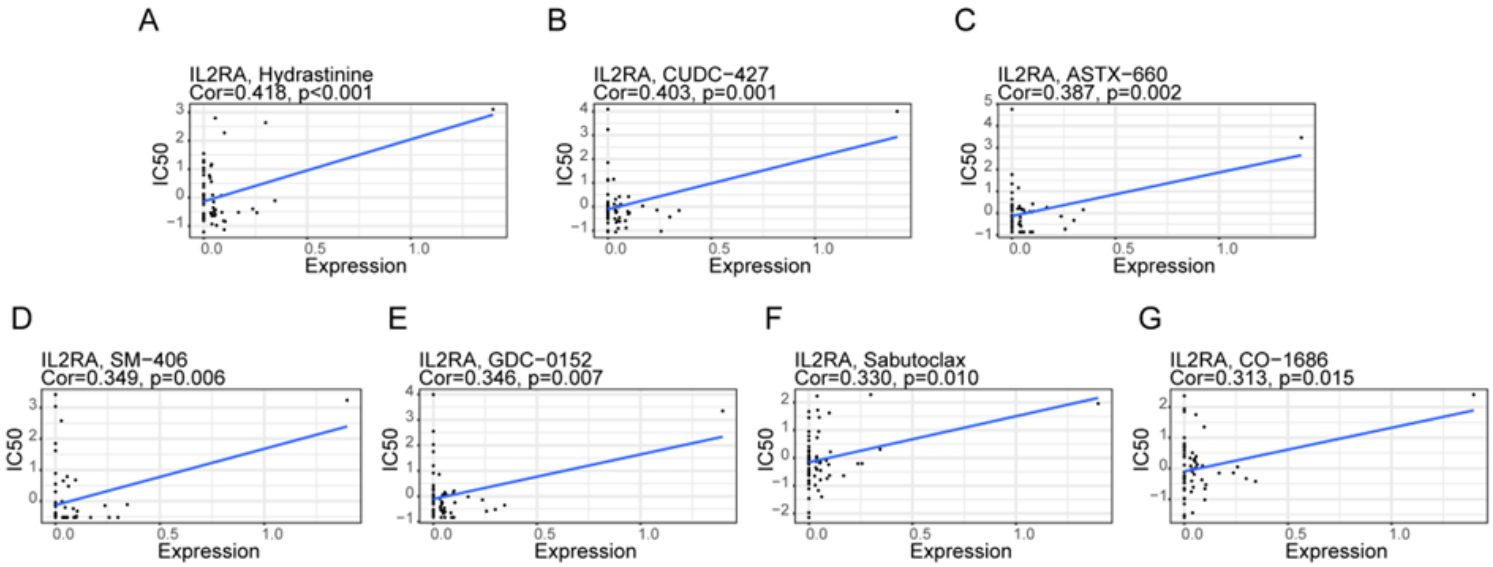


Figure 6

Scatter plot of IL2RA expression and drug sensitivity. (A)Hydrastinine (B)CUDC-427 (C)ASTX-660 (D) SM-406 (E)GDC-1052 (F)Sabutoclax (G)CO-1686

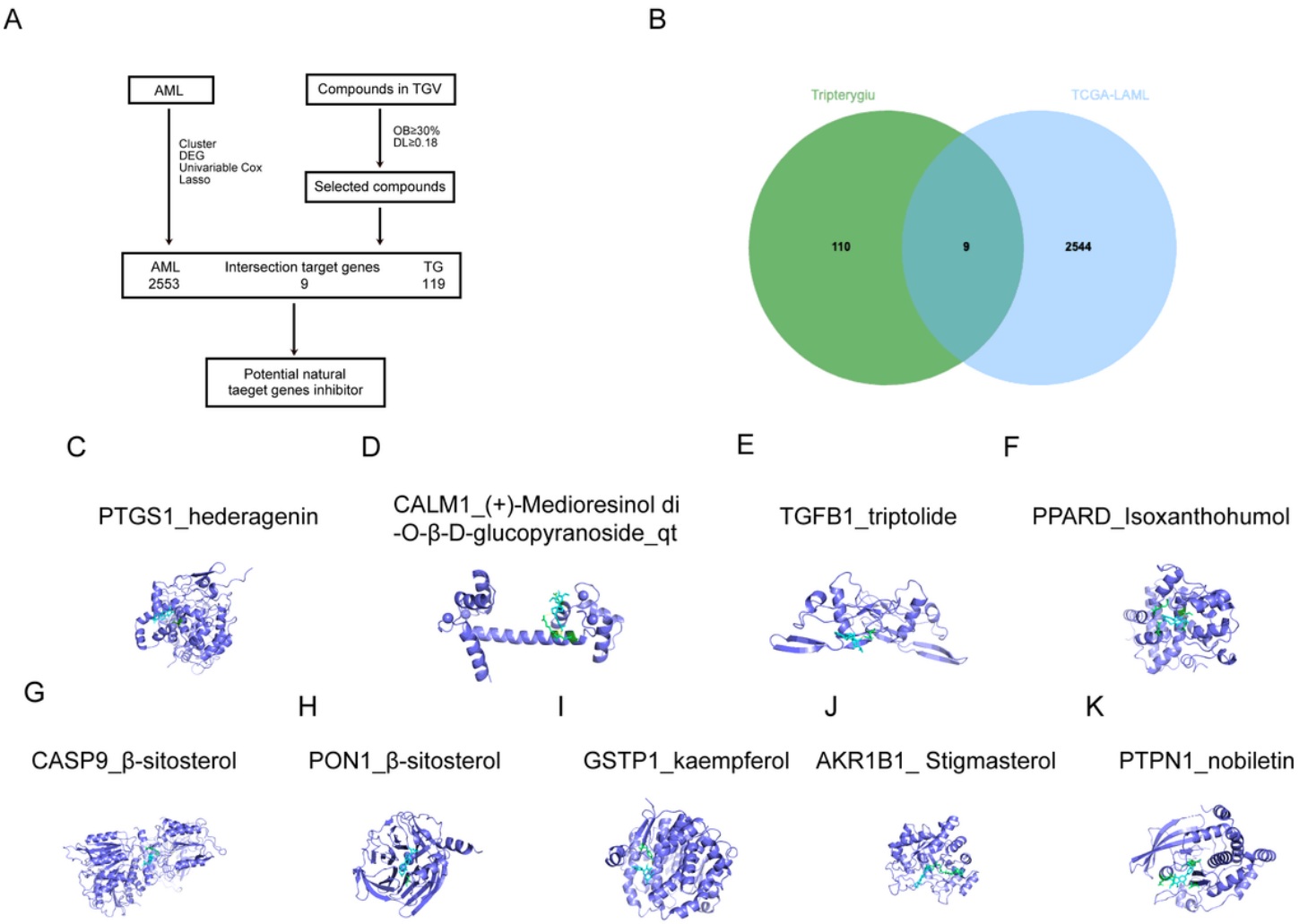


Figure 7

Molecular docking. (A-B The TGV targets in AML (C-K The 3D map of the binding TGV.

A

Drugs	EC50
Hydrastinine	8.653uM
CUDC-427	10.437uM
ASTX-660	1.674nM
GSK-2194069	2.886uM
β-sitosterol	17.476uM

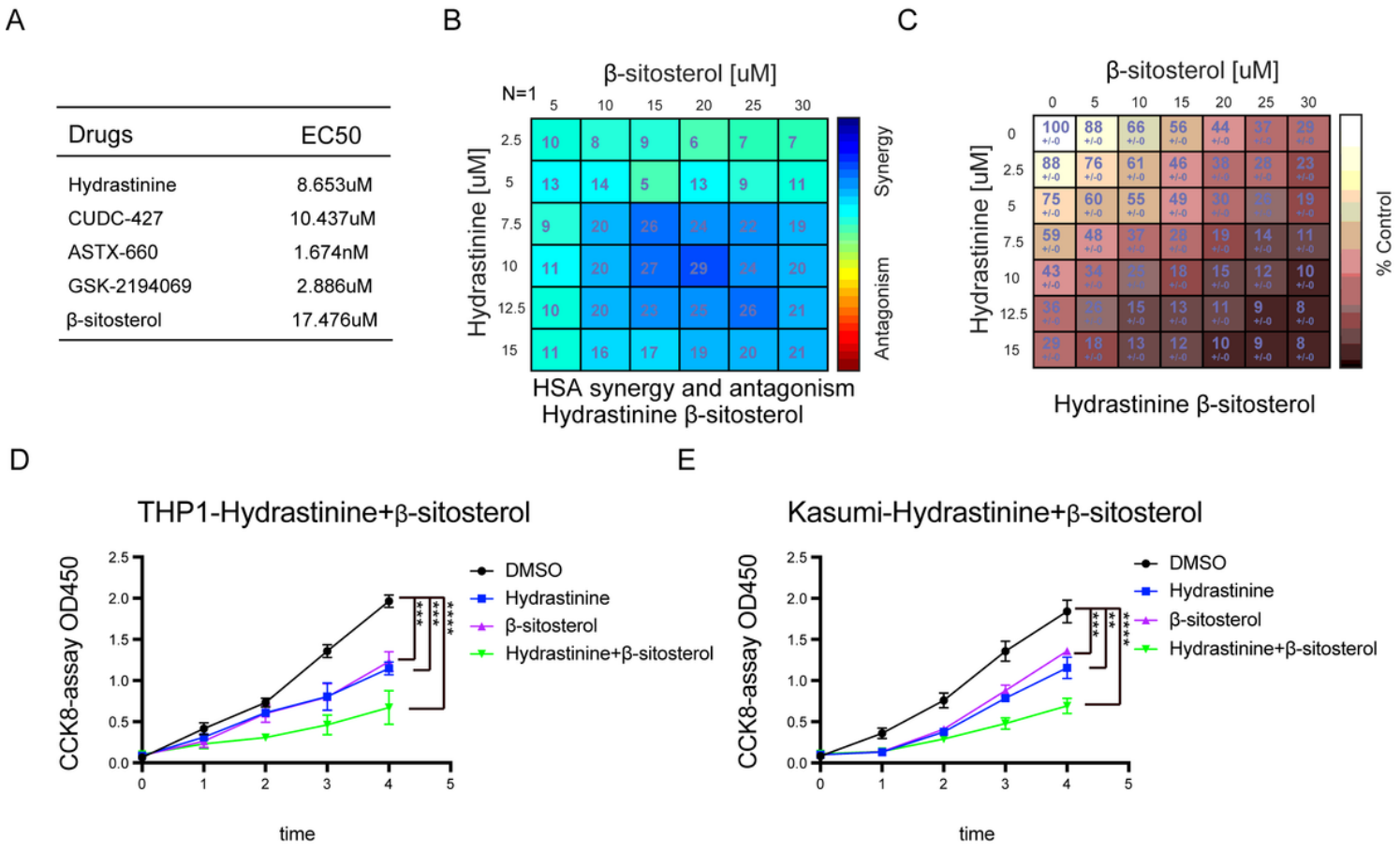


Figure 8

Hydrastinine combined with β-sitosterol has a synergistic antitumor effect on AML

A) The value of EC50 of different drugs.(B-D) The result of a synergistic antitumor in different combination of β-sitosterol and Hydrastinine in THP1 cells. (E)The result of a synergistic antitumor in Kasumi cells.

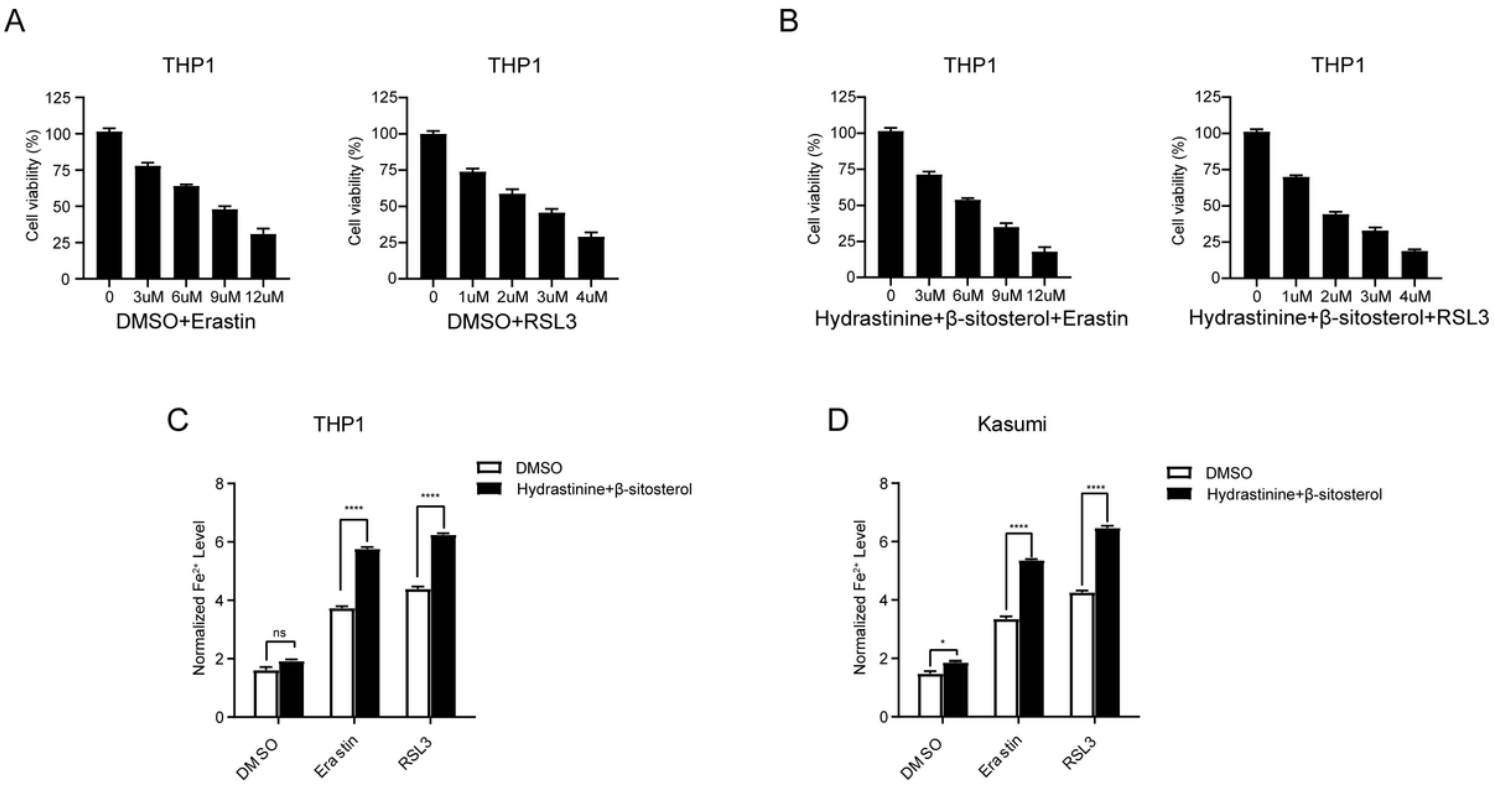


Figure 9

Hydrastinine combined with β-sitosterol enhance the sensitivity of AML cells to ferroptosis inducers A) The CCK8 assay of THP1 cells treating with Erastin and RSLE. (B) The CCK8 assay of THP1 cells treating with Hydrastinine, β-sitosterol, and Erastin or RSL3. (C) The Fe^{2+} levels of THP1 cells with the treatment of DMSO or Hydrastinine and β-sitosteroresult. (D) The Fe^{2+} levels of Kasumi cells with the treatment of DMSO or Hydrastinine and β-sitosteroresult.

Supplementary Files

This is a list of supplementary files associated with this preprint. Click to download.

- Supplementarymaterials.pdf